INTERNATIONAL JOURNAL FOR NUMERICAL AND ANALYTICAL METHODS IN GEOMECHANICS
Int. J. Numer. Anal. Meth. Geomech., **23**, 1175–1194 (1999)

INTERFACE BETWEEN FLUID- AND SOLID-LIKE BEHAVIOUR IN RAPID GRANULAR FLOWS DOWN BUMPY INCLINES

CHUEN-SHII CHOU*

Department of Mechanical Engineering, National Pingtung University of Science and Technology, Pingtung, Taiwan, 91207 Republic of China

SUMMARY

Gravity-driven granular flows down bumpy inclined surfaces were investigated. The flows consist of a bottom region of an amorphous solid-like granular material interacting with a top region of rapidly agitated grains. Chou[1] theoretically analysed these granular flows by employing the constitutive theory,[2] the corresponding boundary conditions[3] and the continuity conditions at the interface.[4] By making use of Chou's model,[1] the research work reported here investigated the effects of the inclination, coefficient of restitution and boundary geometry on the profiles of solid concentration, mean velocity and granular temperature. The direction of the energy flux at the bumpy surfaces, as well as the flow depth for both the active and passive layers were also observed. Copyright © 1999 John Wiley & Sons, Ltd.

KEY WORDS: granular flows; kinetic theory; solid-like; fluid-like; interface; bumpy boundary

1. INTRODUCTION

A granular material is a collection of discrete solid particles immersed in an interstitial fluid and thus, technically, a granular flow is a multiphase process. If the interstitial fluid is a gas, the granular material is said to be dry. When the particles do not adhere to one another, the material is said to be cohesionless. Within the material, these particles may vary in size, shape, orientation, and may be in prolonged or instantaneous contact with their neighbours.

The flow of granular material is an important transport process that occurs in numerous industrial applications and in many geophysical settings. Examples of such granular flows are found in technological processes such as pneumatic transport, powder processing, slurry pipeline, and grain handling in bins and hoppers. Examples of the geophysical phenomena are snow, ice and rock avalanches, mud and debris flow, bed–load transport, the flow of suspended particles in rivers and estuaries, transport of dust and the transport of sediment and ice in rivers and oceans.

The mechanical behaviour of dry, cohesionless granular material can be classified into rate-dependent (rapid flow), transitional and quasi-static (slow flow) regimes. In the rapid flow regime,

* Correspondence to: Chuen-Shii Chou, Department of Mechanical Engineering, National Pingtung University of Science and Technology, Pingtung, Taiwan 91207, Republic of China. E-mail: cschou@mail.npust.edu.tw

Contract/grant sponsor: National Science Council, Republic of China; contract/grant number: NSC-84-2212-E-020-002

CCC 0363–9061/99/121175–20$17.50

Received 20 May 1997
Revised 21 November 1997 and 7 July 1998

the principal transport mechanisms are kinetic transport by particle fluctuations and collisional transport due to particle interactions. In the quasistatic regime, the principal transport mechanism occurs through the network of contact force created by the continuous and simultaneous contact among the particles.

Recent reviews of rapid (or rate-dependent) granular flows have been compiled by Savage[5] in which continuum theories, microstructural theories, numerical modelling and rheological test devices and experiments were discussed briefly, Richman[6] discussed the kinetic theories that govern the flow of granular material and the corresponding boundary conditions, Campbell[7] discussed various modelling techniques used to describe the motion of the bulk material, Haff[8] presented a physical and heuristic discussion of the kinetic model for granular fluids, and Jenkins[9] reviewed recent theories for idealized granular materials experiencing rapid deformation. On the other hand, Hutter and Rajagopal[10] reviewed the behaviour of a material made up of a large assemblage of solid particles under rapid and quasi-static deformations.

Experimental investigations of gravity-driven granular flows have been carried out by Takahasi,[11] Bagnold,[12] Augenstein and Hogg,[13] Hungr and Morgenstern,[14] Ahn *et al.*,[15,16] Johnson *et al.*,[17] Drake,[18] Ishida and Shirai,[19] Dolgunin and Ukolov,[20] Nott and Jackson,[21] Hutter *et al.*,[22] Roberts.[23]

Theoretical investigations of gravity-driven granular flow have been carried out by Savage,[24] Ahmadi and Shahinpoor,[25] Sayed and Savage,[26] Ma and Ahmadi,[27] Hutter *et al.*,[28,29] Johnson *et al.*,[17] Richman and Marciniec,[30] Ahn *et al.*,[31] Dolgunin and Ukolov,[20] Haff,[32] Nunziato and Passman,[33] Anderson and Jackson,[34] Nott and Jackson,[21] Savage and Hutter,[35,36] Hutter,[37] Lang,[38] Perla *et al.*,[39] Norem *et al.*,[40] Rajagopal and Gudhe,[41] and Chou.[1] By using numerical simulation, Campbell and Brennen,[42] Campbell *et al.*,[43] Walton *et al.*,[44] and Norem *et al.*,[45] analysed chute flows. Szidarovszky *et al.*,[46] numerically studied the steady plane granular chute flows by using the Jenkins–Savage model.

The gravity-driven granular flows which consist of a bottom fluidized layer interacting with a top passive layer are treated in detail in References 17, 28 and 29. On the other hand, Takahasi[11] performed an investigation of chute flows. Tests were made using dry sands of various sizes flowing down a straight channel of rectangular cross-section that could be set at different inclinations. He noticed two modes of flow: one, which consisted of an upper thin layer of particles flowing over a stationary layer overlying the chute bed; and a second, where all the particles were in motion, each particle following a chaotic fluctuating path and interacting vigorously with its neighbours. Takahasi drew attention to the similarities between these experiments and the natural phenomena such as snow avalanches and land slides.

By employing the constitutive theory,[2] the corresponding boundary conditions[3] and the continuity conditions at the interface,[4] Chou[1] theoretically analyzed granular chute flows consisting of a bottom passive layer and a top active layer shown in Figure 1. By making use of Chou's model,[1] we investigated the effects of the inclination, coefficient of restitution and boundary geometry on the profiles of solid concentration, mean velocity and granular temperature. The variations of energy flux with boundary geometry and the flow depth for both the active and passive layers were observed, too.

2. KINETIC THEORY

In developing recent theories for the rapid flowing of granular materials, workers have exploited the analogy between the fluctuating nature of rapid granular motion and the random molecular

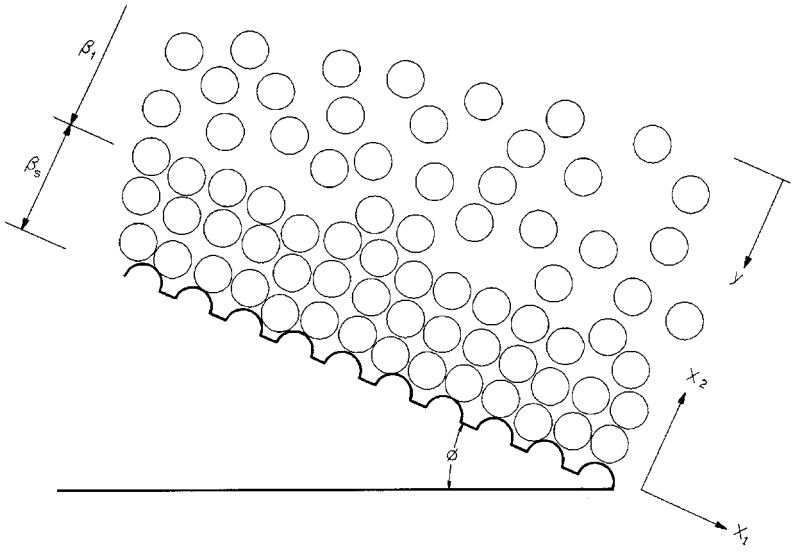

Figure 1. Gravity-driven granular flows

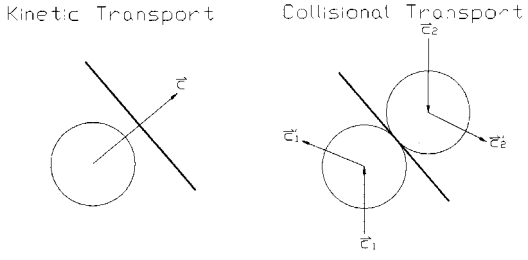

Figure 2. A schematic drawing of particle's kinetic transport mode and collisional transport mode

motion within a dense gas. The grains are assumed to interact vigorously with their neighbours through energy dissipating binary collisions, while the effects of enduring contacts and static friction between grains are ignored. Considering a statistical description of the particles' velocities, it is possible to define mean fields such as density, velocity and granular temperature and to derive balance equations corresponding to each. Constitutive quantities may then be identified through their appearance in these balance equations and constitutive relations may be obtained through appropriate statistical averaging. The appearance in these constitutive theories of a rate of dissipation due to inelastic collisions is the most striking departure from the kinetic theory for dense gases. In the rapid granular flow regime, the principal transport mechanisms are kinetic transport by particle fluctuations and collisional transport due to particle interactions. A schematic drawing of kinetic transport between collisions and collisional transport between two particles is shown in Figure 2.

2.1. Balance equations

The mean fields necessary to describe the granular flow of nearly elastic smooth spheres with velocity $\mathbf{c}$ are solid fraction v (or mass density of flow ρ), mean velocity of flow $\mathbf{u}$ and granular temperature T, that is, the kinetic energy per unit mass associated with fluctuation velocity. The fluctuation velocity $\mathbf{C}$ is defined as the difference $\mathbf{c} - \mathbf{u}$. By referring to a direct analysis of the flow through a differential control volume fixed in space,[47] the general governing equation for the rate of change of the mean amount $\langle n\psi \rangle$ of particle property $\psi(\mathbf{c})$ within the volume element is

$$\frac{\partial \langle n\psi \rangle}{\partial t} = n\mathbf{g} \cdot \left\langle \frac{\partial \psi}{\partial \mathbf{c}} \right\rangle - \nabla \cdot \langle n\mathbf{c}\psi \rangle + \aleph(\psi) \tag{1}$$

Here $\mathbf{g}$ is the body force per unit mass and $\aleph(\psi)$ is the rate of change of ψ per unit volume due to collisions. Equation (1) expresses the fact that at any fixed spatial location, the rate of change of $\langle n\psi \rangle$ occurs due to three facts: (i) the external force (e.g. body force acting on each particle to change $\mathbf{c}$ and therefore $\psi(\mathbf{c})$), (ii) the net flux of particles bearing the property $\psi(\mathbf{c})$ into the volume element and (iii) the collisional production of ψ which may be decomposed into the sum

$$\aleph(\psi) = \chi(\psi) - \nabla \cdot \boldsymbol{\theta}(\psi) \tag{2}$$

Equation (2) has been shown by Jenkins and Savage.[48] In this decomposition, $\chi(\psi)$ and $\boldsymbol{\theta}(\psi)$ are the collisional source term and the collisional flux term respectively. Both $\chi(\psi)$ and $\boldsymbol{\theta}(\psi)$ are expressible as integrals over all possible collisions. They are essentially statistical averages of the change per collision in the appropriate particle properties weighed by the frequency of each collision. The frequency of each collision is related to the pair distribution function at impact, and the pair distribution function depends on two particles' velocities and positions.

With $\psi = m$ in equation (1), the balance equations for mass becomes

$$\dot{\rho} + \rho \nabla \cdot \mathbf{u} = 0 \tag{3}$$

where an overdot denotes the derivative while traveling with the mean flow.

Similarly, taking ψ in equation (1) equal to $m\mathbf{c}$ and eliminating the intermediate results using equation (3), the balance equation for momentum becomes

$$\rho \dot{\mathbf{u}} = -\nabla \cdot \boldsymbol{P} + \rho \mathbf{g} \tag{4}$$

the negative sign indicates that the compressive stress acts on the granular material, therefore $\boldsymbol{P}$ is called the pressure tensor by most researchers. The pressure tensor $\boldsymbol{P}$ measures the flux of momentum within the flow and is the sum for a collisional contribution $\boldsymbol{\theta}(m\mathbf{C})$ and a particle kinetic transport contribution $\langle \rho \mathbf{CC} \rangle$. A collisional source term does not appear here because linear momentum is conserved in binary collisions.

The balance equation for the energy associated with velocity fluctuations, found by setting $\psi = mc^2/2$, replacing $\langle C^2 \rangle/3$ with granular temperature T and eliminating the intermediate results using equations (3) and (4), is provided by

$$\frac{3}{2} \rho \dot{T} = -\nabla \cdot \mathbf{Q} - \mathrm{tr}(\boldsymbol{P} \cdot \nabla \mathbf{u}) - \gamma \tag{5}$$

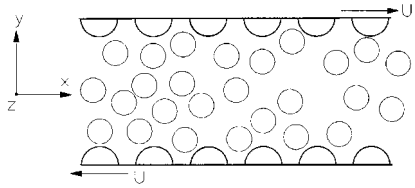

Figure 3. The steady simple shear granular flow driven by the relative motion of two identical parallel bumpy boundaries

Where $\mathbf{Q}$ is the flux of the kinetic energy associated with the velocity fluctuations and $\gamma = -\chi(mC^2/2)$ is the rate per unit volume at which energy becomes dissipated due to inelastic collision. In general, the energy flux $\mathbf{Q}$ is composed of contributions coming from particle collisions as well as from the kinetic transport of particles between collisions. Consequently, the total energy flux $\mathbf{Q}$ is the sum of the collisional part of the energy flux vector $\boldsymbol{\theta}(mC^2/2)$ and the kinetic transport part of the energy flux vector $\langle \rho \mathbf{C} C^2/2 \rangle$.

In order to clearly explain the second term on the right-hand side of equation (5), a steady, fully developed, rectilinear shear flow shown in Figure 3 is illustrated. The upper boundary moves in the x-direction with a constant speed U while the lower boundary moves with the same speed in the opposite direction. The velocity u in the x-direction and the solid fraction v are functions of y only. The granular temperature is assumed to be constant throughout the flow. In this case, the balance of mass equation (3) is satisfied identically. In the absence of gravity, the x- and y-momentum balance equation (4) may be integrated to show that both P_{xy} and P_{yy} are constant. The energy balance equation (5) is reduced to $-P_{yx}(\mathrm{d}u/\mathrm{d}y) = \gamma$, therefore, the stress power generated by moving the upper and lower walls is dissipated by inelastic binary collisions in order to maintain a steady flow.

2.2. Constitutive theory

The constitutive theory of Jenkins and Richman[2] for the granular flows of identical, smooth, nearly elastic spheres of diameter σ and mass density of particle ρ_{p} (i.e. $\rho_{\mathrm{p}} = \rho/v$) is employed here. The constitutive theory is employed here which includes the statistically averaged effects of particle kinetic transport between collisions and binary collisions between particles. Consequently, this theory is not restricted to dense flows where a collisional mode dominates the transport mechanisms. The constitutive quantities: the pressure tensor $\boldsymbol{P}$; the flux of kinetic energy associated with the velocity fluctuation $\mathbf{Q}$; and the rate per unit volume at which the energy is dissipated due to inelastic collisions γ are given, respectively, by

$$\boldsymbol{P} = (4\rho GFT)\boldsymbol{I} - (2\mu E)\hat{D} \tag{6}$$

$$\mathbf{Q} = -\frac{5\mu M \nabla T}{2} \tag{7}$$

and

$$\gamma = \frac{15\mu(1-e)T}{\sigma^2} \tag{8}$$

Where e is the coefficient of restitution, $\hat{D}$ is the deviatoric part of $(\nabla\mathbf{u} + \nabla\mathbf{u}^{\mathrm{T}})/2$, $F(v) = 1 + 1/4G$, $E(v) = 1 + \pi(1 + 5/8G)^2/12$, $M(v) = 1 + 9\pi(1 + 5/12G)^2/32$, $G(v) = v(2 - v)/1(1 - v)^3$, and $\mu = (8\sigma\rho G\sqrt{(\mathrm{T})})/(5\sqrt{(\pi)})$. This constitutive theory applies only to circumstances in which $(1 - e)$ is of the same order as $\varepsilon = \sigma/L$, where L is a characteristic length over which the mean fields vary. Finally, we point out that the constitutive theory admits all values for solid fractions that are less than one. This is because the expression for the frequency of collisions employed in deriving the theory was based upon the radial distribution function of Verlet and Levesque,[49] which diverges only when $v = 1$, but which gives reasonable results for all values of v up to the value at which enduring contacts dominate particle interactions.

2.3. Boundary conditions

The bumpy surface with a unit inward **n**, a flat wall to which identical smooth hemispherical particles of diameter d are randomly attached at an average distance s apart, is shown in Figure 4. The balance of the momentum and the energy at the bumpy boundary derived by Richman[3] are given, respectively, by

$$\mathbf{M} = \boldsymbol{P}\cdot\mathbf{n} \tag{9}$$

and

$$\mathbf{M}\cdot\mathbf{v} - D = \mathbf{Q}\cdot\mathbf{n} \tag{10}$$

Where **M** is the rate of momentum per unit area supplied to the flow by the boundary through collisions, D is the rate of energy per unit area absorbed from the flow and **v** is the slip velocity obtained by subtracting the flow velocity at the boundary from the velocity of the boundary. The slip-work term $M\cdot\mathbf{v}$ is due to equal traction on the opposite sides of the rectangle acting through velocities that differ by an amount **v**. This is the mechanism by which the boundaries may supply fluctuation energy to the flow, although it is the relative magnitude of the slip work and the dissipation rate D that ultimately determines the direction of the energy flux normal to the boundary. When these two balance exactly, the boundary neither supplies nor absorbs energy from the flow. Expressions for **M** and D, in terms of the mean fields, depend on the geometry and dissipative character of the boundary.

If dimensionless measures for wall geometry $r = \sigma/d$ and $\Delta = s/d$ are defined, then the fraction of the surface area of each wall particle that is accessible to a flow particle is $(1 - \cos\theta)$, where $\sin\theta = (1 + \Delta)/(1 + r)$. Consequently, $\sin\theta$ appears to be a natural measure of wall roughness. The Δ must necessarily be less than $-1 + \sqrt{(1 + 2r)}$ so as to ensure that no flow particles ever

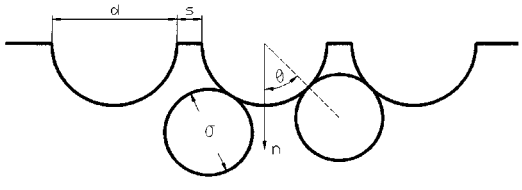

Figure 4. Boundary geometry

collide with the flat part of the wall. When Δ is between 0 and $-1+\sqrt{(1+2r)}$, the boundary may be made effectively rougher either by increasing Δ or by decreasing r. The coefficient of restitution between the wall particles and flow particles is e_w, and $(1-e_w)$ is of order ε. When a flow particle collides with a wall particle, the distance between their centre is $\bar{\sigma}=(\sigma+d)/2$.

The resulting Cartesian components of $\mathbf{M}^3$ are

$$M_i=\rho\chi T\left\{n_i+\sqrt{\left(\frac{2}{\pi}\right)}\frac{2v_i}{3\sqrt{T}}[2\csc^2\theta(1-\cos\theta)-\cos\theta]\right.$$
$$\left.+\sqrt{\left(\frac{2}{\pi}\right)}\frac{\bar{\sigma}u_{kj}}{\sqrt{(T)}}\left[\left(1+\frac{\sigma B}{\bar{\sigma}}\right)I_{ijk}+n_jI_{ik}\right]\right\} \tag{11}$$

in which

$$B(\nu)=\frac{\pi}{12\sqrt{(2)}}\left(1+\frac{5}{8G}\right) \tag{12}$$

Here a comma denotes differentiation with respect to the co-ordinates of position and the factor $\chi(\nu)$ accounts for the effects of excluded volume and the shielding of flow particles from the wall particles by other flow particles. The tensor components I_{ik} and I_{jk} depend on the boundary geometry and are defined by

$$I_{ik}=\tfrac{2}{3}\{2[\csc^2\theta(1-\cos\theta)+\cos\theta]n_in_k+[2\csc^2\theta(1-\cos\theta)-\cos\theta](z_iz_k+t_it_k)\} \tag{13}$$

where **t**, **z** and **n** form an orthonormal triad, and

$$I_{ijk}=(\sin^2\theta-2)n_in_jn_k-\tfrac{1}{2}\sin^2\theta[n_i(z_jz_k+t_jt_k)+n_j(z_kz_i+t_kt_i)+n_k(z_iz_j+t_it_j)] \tag{14}$$

In order to explain the application of equations (11), (13) and (14), we illustrate a steady rectilinear shear flow shown in Figure 3. In this case, **n** points to the negative y direction and **t** points to the x direction. Consequently, t_x and $-n_y$ are equal to 1. For the x-component of **M**, both the subscripts i nd k are equal to x and subscript j is equal to y. Therefore I_{xx} and I_{xyx} reduce to $2[2\csc^2\theta(1-\cos\theta)-\cos\theta]/3$ and $\sin^2\theta/2$, respectively.

The expression for D^3 is given using

$$D=2\sqrt{\left(\frac{2}{\pi}\right)}(1-e_w)\csc^2\theta(1-\cos\theta)\rho\chi T^{3/2} \tag{15}$$

2.4. Compatibility conditions for the interface

We consider gravity-driven granular flows down bumpy inclined surfaces. The flows consist of a bottom region of an amorphous (or glassy) solid-like granular material, in which the mean velocity gradient vanished but collisions between particles persist, interacting with a top region of rapidly agitated grains. We refer to the concept of continuity at the interface indicated by Jenkins and Askari;[4] the fluctuation energy must be continuous across the interface as well as the solid fraction must be continuous in order to provide continuity of the normal traction. The transition conditions at the interface employed in Section 3.5 are (i) the fluctuation energy continuity condition and (ii) the fluctuation energy flux continuity condition.

3. STEADY GRAVITY-DRIVEN GRANULAR FLOWS HAVING ACTIVE AND PASSIVE LAYERS

By employing the constitutive theory[2] (see Section 2.2), the corresponding boundary conditions[3] (see Section 2.3) and the continuity conditions at the interface[4] (see Section 2.4), Chou[1] theoretically analysed granular chute flows consisting of a bottom passive layer and a top active layer shown in Figure 1. By making use of Chou's model[1] for nearly elastic, smooth, and identical spheres, a boundary-value problem is constructed. We replace the solid fraction v_f in the fluid-like region and solid fraction v_s in the solid-like region using their depth-averaged values $\bar{v}_f$ and $\bar{v}_s$ in order that the analytical (but not exact) expressions of granular temperature for both the active and passive layers may be obtained from fluctuation energy equations. Unknown constant coefficients in the expressions of granular temperature may be determined numerically by employing boundary conditions at the bumpy base and compatibility conditions at the interface.

3.1. Description of steady gravity-driven flows

The gravity-driven flows shown in Figure 1 consist of a bottom region of an amorphous solid-like granular material interacting with a top region of rapidly agitated grains. A Cartesian coordinates system x_1–x_2–x_3 and the vertical acceleration g due to gravity are introduced, x_1 measures parallel distances along the inclined bumpy surfaces located at an angle ϕ from the horizontal and x_2 measures perpendicular distance above the incline. The flow depth of the fluid-like region is β_f and the flow depth of the solid-like region is β_s. L is defined as the perpendicular distance from the incline to the free surface which is the sum of β_f nd β_s. If $y = (L - x_2)/\sigma$ is the dimensionless co-ordinate measured from the free surface and the flows are infinitely extended in the x_3-direction, then the solid fraction v, the dimensionless velocity $u = u_1/(\sigma g)^{1/2}$ and the dimensionless granular temperature $w = (T/\sigma g)^{1/2}$ depend on y only. Consequently, in this steady gravity-driven flow, equation (3) and the x_3-component of equation (4) are satisfied identically.

3.2. Dimensionless momentum and energy equations

In terms of dimensionless quantities: normal stress $N = P_{22}/(\rho_p \sigma g)$; shear stress $S = -P_{12}/(\rho_p \sigma g)$; energy flux $q = Q_2/[\rho_p(\sigma g)^{3/2}]$, and energy dissipation $\Gamma = \gamma/(\rho_p \sqrt{(\sigma g^3)})$, the x_1 and x_2 components of equation (4) as well as equation (5) are, respectively, reduced to

$$\frac{dS}{dy} = v \sin\phi \tag{16}$$

$$\frac{dN}{dy} = v \cos\phi \tag{17}$$

and

$$\frac{dq}{dy} - S\frac{du}{dy} - \Gamma = 0 \tag{18}$$

From equations (16) (17), the stress variations in both the active and passive layers could be determined provided the solid fraction profiles for both the layers are known.

By substituting the dimensionless constitutive quantities: shear stress $S = -\eta E(\mathrm{d}u/\mathrm{d}y)$; energy flux $q = [2MN(\mathrm{d}w/\mathrm{d}y)]/(\sqrt{(\pi)}F)$; energy dissipation $\Gamma = [6(1-e)Nw]/(\sqrt{(\pi)}F)$, and viscosity $\eta = \mu/(\rho_{\mathrm{p}}\sqrt{(\sigma^3 g)})$ into equation (18), the energy equation for a full range of solid fractions may be written in terms of the dimensionless granular temperature w and its derivatives through

$$\frac{w''}{w} + \left[(1-2H)\frac{N'}{N}\right]\frac{w'}{w} + 4H\left(\frac{w'}{w}\right)^2 - \lambda^2 = 0 \tag{19}$$

in which λ^2 is defined by

$$\lambda^2 = \frac{[6(1-e) - (5\pi F^2/2E)(S/N)^2]}{2M} \tag{20}$$

and H, which is the function of solid fraction, is given using

$$H = \frac{1}{2}\frac{(\mathrm{d}/\mathrm{d}v)[\ln(F/M)]}{(\mathrm{d}/\mathrm{d}v)[\ln(vGF)]} \tag{21}$$

and $S/N = \tan\phi$.

In the dense limit, since H and the mean velocity gradient vanish, the energy equation for solid-like granular flows (passive layer) is given from equation (19) using

$$\frac{w''}{w} + \left(\frac{N'}{N}\right)\frac{w'}{w} - \Lambda^2 = 0 \tag{22}$$

where $\Lambda^2 = 3(1-e)/M$.

3.3. Granular temperature profiles

In order to simplify the solution procedure and obtain analytical (but not exact) expressions for granular temperature, for both the active and passive layers, we replace v_{f} with its depth-averaged value $\bar{v}_{\mathrm{f}}$ in fluid-like region, and replace v_{s} with its depth-averaged value $\bar{v}_{\mathrm{s}}$ in solid-like region. The $\bar{v}_{\mathrm{f}}$ and $\bar{v}_{\mathrm{s}}$ are defined, respectively, by

$$\bar{v}_{\mathrm{f}} = \frac{1}{\beta_{\mathrm{f}}}\int_0^{\beta_{\mathrm{f}}} v_{\mathrm{f}}\,\mathrm{d}y \text{ and } \bar{v}_{\mathrm{s}} = \frac{1}{\beta_{\mathrm{s}}}\int_{\beta_{\mathrm{f}}}^{\beta_{\mathrm{f}}+\beta_{\mathrm{s}}} v_{\mathrm{s}}\,\mathrm{d}y \tag{23}$$

By integrating equation (17) and eliminating the integrating constant with the condition that there is no stress acting on the free surface, we obtain $N = y\bar{v}_{\mathrm{f}}\cos\phi$. Therefore, the ratio of N' to N is equal to $1/y$ and the energy equation (19) then becomes

$$\frac{w''}{w} + \left[(1-2H)\frac{1}{y}\right]\frac{w'}{w} + 4H\left(\frac{w'}{w}\right)^2 - \lambda^2 = 0 \tag{24}$$

in which H and λ are evaluated at $\bar{v}_{\mathrm{f}}$. Equation (24) is a Riccati equation of w'/w, which is equivalent to a modified Bessel equation of order H for the variation of w^{1+4H}/y^H with $(\lambda\sqrt{1+4H})y$. The solution for equation (24) found by Richman and Marciniec[30] is given using

$$w_{\mathrm{f}}(y) = A[y^H I_{-H}(ky)]^{1/(1+4H)} \tag{25}$$

where I_{-H} is the modified Bessel function of order $-H$, k^2 is equal to $(1+4H)\lambda^2$, and A is a positive constant to be determined. Equation (25) applies when λ^2 is positive. In this case, the

rate at which the energy is dissipated due to inelastic collisions between flow particles in the fluid-like granular flow is greater than the rate at which energy is supplied by gravity. On the other hand, the solution for equation (24) for which λ^2 is negative is given using

$$w_f(y) = A[y^H J_{-H}(Ky)]^{1/(1+4H)} \tag{26}$$

where J_{-H} is the Bessel function of order $-H$, and K^2 is equal to $-(1+4H)\lambda$. In this case, the rate at which the energy is dissipated due to inelastic collisions between flow particles in the fluid-like granular flow is less than the rate at which the energy is supplied by gravity.

By replacing v_s with its depth-averaged value $\bar{v}_s$ in the solid-like region, integrating equation (17) and eliminating the integrating constant with the stress continuity condition at the interface $y = \beta_f$, we obtain $N = y\bar{v}_s \cos\phi + \beta_f(\bar{v}_f - \bar{v}_s)\cos\phi$. Therefore, the ratio of N' to N is equal to $1/(y - \beta_f(1 - \bar{v}_f/\bar{v}_s))$ and the energy equation (22) for the solid-like granular flow is reduced to

$$w'' + \frac{1}{z}w' - \Lambda^2 w = 0 \tag{27}$$

in which z is equal to $y - \beta_f(1 - \bar{v}_f/\bar{v}_s)$ and Λ is evaluated at $\bar{v}_s$. Equation (27) can be rearranged to be another simple second-order ordinary differential equation, as follows:

$$Y^2 \frac{d^2W}{dY^2} + Y\frac{dW}{dY} - Y^2 W = 0 \tag{28}$$

where $W = w$ and $Y = z\Lambda$. By employing the power series method, the solution for equation (28) is

$$W_s(Y) = B_1 I_0(Y) + B_2 K_0(Y) \tag{29}$$

where I_0 is the modified Bessel function of the first kind of order zero, K_0 is the modified Bessel function of the third kind of order zero and B_1 as well as B_2 are unknown constants to be determined.

3.4. Solid fraction profiles

The constitutive relation for normal stress in dimensionless form is given using

$$N = 4\nu GFw^2 \tag{30}$$

By substituting the normal stress $N = y\bar{v}_f \cos\phi$ for an active layer into equation (30), an equation to determine the solid fraction profile $v_f(y)$ in the fluid-like region is given as follows:

$$y\bar{v}_f \cos\phi - 4v_f G(v_f)F(v_f)w_f^2 = 0 \tag{31}$$

By substituting the normal stress $N = y\bar{v}_s \cos\phi + \beta_f(\bar{v}_f - \bar{v}_s)\cos\phi$ for a passive layer into equation (30), an equation to determine the solid fraction profile $v_s(y)$ in the solid-like region is obtained as follows:

$$y\bar{v}_s \cos\phi + \beta_f(\bar{v}_f - \bar{v}_s)\cos\phi - 4v_s G(v_s)F(v_s)W_s^2 = 0 \tag{32}$$

If the granular temperature profiles for both the active and passive layers are known, the solid fraction profiles $v_f(y)$ and $v_s(y)$ may be obtained through an iterative method (e.g. Newton–Raphson method).

3.5. Solving flow depths and unknown integrating constants

The dimensionless flow depths β_f and β_s as well as the unknown constants A, B_1 and B_2 are determined using equation (23), fluctuation energy compatibility condition at the interface

$$w_f(\beta_f) = W_s(\beta_f) \tag{33}$$

fluctuation energy flux compatibility condition at the interface

$$\frac{w'_f(\beta_f)}{w_f(\beta_f)} = \frac{W'_s(\beta_f)}{W_s(\beta_f)} \tag{34}$$

and the fluctuation energy flux boundary condition at the bumpy surface

$$\frac{W'(\beta_f + \beta_s)}{W(\beta_f + \beta_s)} = b \tag{35}$$

in which

$$b = \frac{F}{\sqrt{2M}}\left[\frac{\pi}{2}\left(\frac{S}{N}\right)^2 f_b - 2(1 - e_w)(1 - \cos\theta)\csc^2\theta\right] \tag{36}$$

and

$$f_b = \frac{3}{2[2(1 - \cos\theta)\csc^2\theta - \cos\theta]} \tag{37}$$

Equation (35) is obtained by employing equation (10), the boundary condition of the balance of energy at the bumpy surface.

For positive λ^2 as well as the fixed values for $\bar{\nu}_f$, $\bar{\nu}_s$, e, e_w, r, Δ and ϕ, we employ equation (25) in equation (34), substitute equation (29) into equation (35), then simultaneously solve these two intermediate equations with appropriate initial guesses B_1 and β_f. Consequently, B_2 and β_s are determined and by substituting equation (25), B_1, B_2, and β_f into equation (33), A is obtained. As a check on the initial guesses of β_f and B_1, we calculate the depth-average values for solid fractions for both the fluid- and solid-like regions according to equation (23) and compare these to $\bar{\nu}_f$ and $\bar{\nu}_s$ that were chosen originally. After a suitable number of iterations on β_f and B_1 to ensure good agreement with $\bar{\nu}_f$ and $\bar{\nu}_s$, the finalized profiles of solid fraction and granular temperature for both the fluid- and solid-like regions are obtained.

For negative λ^2, the solution procedure is identical except using equation (26) instead of equation (25). The final boundary condition, balance of momentum at the bumpy surface, will be used to obtain the slip velocity v at the inclined bumpy surface. Finally the dimensionless velocity profile $u(y)$ and mass flow rate $\dot{m}$ are given, respectively, using

$$u = \mathrm{v} + \frac{5\sqrt{(\pi)}S}{2N}\int_y^{\beta_f} \frac{F}{E}\, w_f(\xi)\, \mathrm{d}\xi \tag{38}$$

and

$$\dot{m} = \int_0^{\beta_f} \nu_f u_f\, \mathrm{d}y + \int_{\beta_f}^{\beta_f + \beta_s} \nu_s u_s\, \mathrm{d}y \tag{39}$$

The flow chart of calculations is shown in Figure 5.

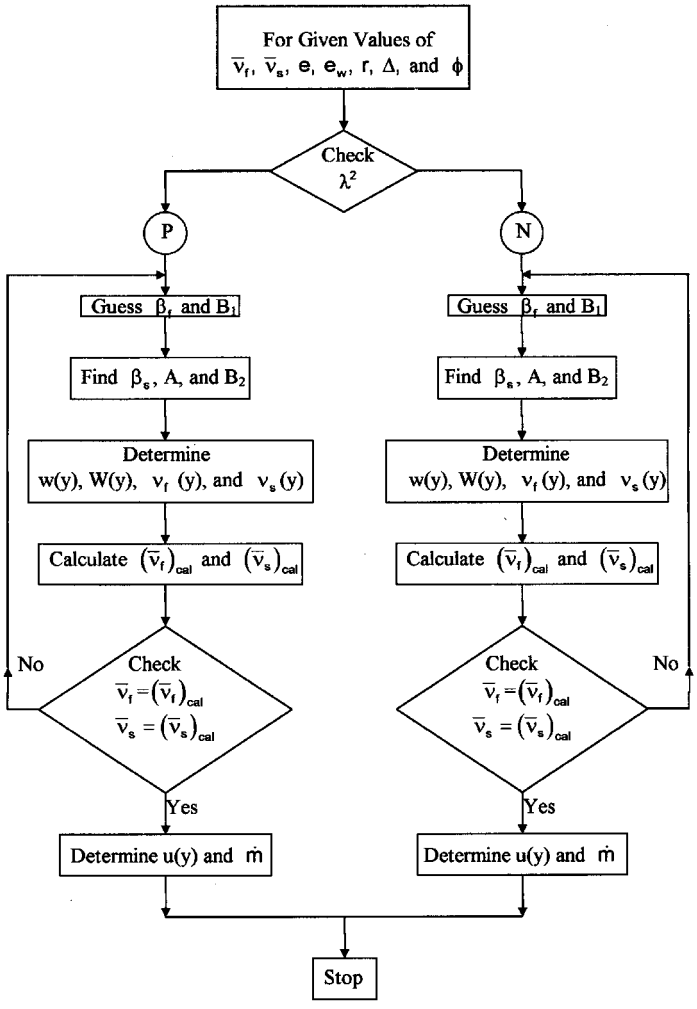

Figure 5. Flow chart of calculations

4. RESULTS AND DISCUSSIONS

4.1. $(1 - e_w)/(1 - e)$ versus ν

When the boundary neither supplies nor absorbs flows of non-zero depth, the neutral cases (homogeneous flows) occur and the granular temperature is constant throughout the flows. In Figure 6, the dependence of the ratio $(1 - e_w)/(1 - e)$ on ν is shown for $\Delta = 0$ and $r = \frac{1}{2}, \frac{3}{4}, 1$ and $\frac{4}{3}$. The curves represent the neutral cases ($\lambda^2 = 0$), the area below each curve corresponds to the circumstances under which the boundary supplies energy to the flows and the area above each curve corresponds to circumstances under which the boundary absorbs energy. For a fixed value of the coefficient of restitution between flow particles e, an increase in the value of $(1 - e_w)/(1 - e)$

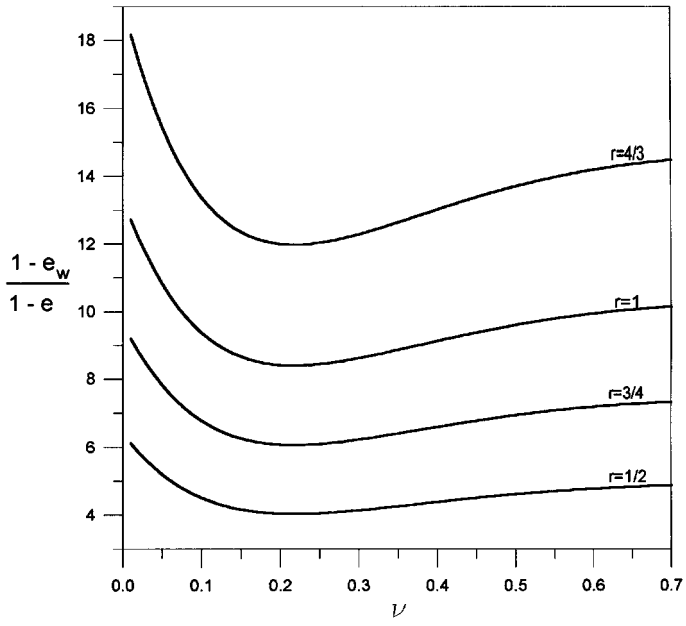

Figure 6. The dependence of the ratio $(1 - e_w)/(1 - e)$ on v for $\Delta = 0$ and $r = \frac{1}{2}, \frac{3}{4}, 1$ and $\frac{4}{3}$

corresponds to an increase in the inelasticity of wall-flow particle collisions. This results, consequently, in more circumstances under which the boundary absorbs energy. The boundary evolves from a fluctuation energy supplier to an absorber. The dimensionless measure of wall geometry r is the ratio of the diameter of a flow particle to that of a wall particle. As the values of diameter for wall particles and the distance between the wall particles are fixed, the boundary becomes smoother provided r is increasing. This consequently results in greater slip work ($\mathbf{M}\cdot\mathbf{v}$), and then more circumstances under which the boundary supplies energy.

In Figure 7, the dependence of the ratio $(1 - e_w)/(1 - e)$ on v is shown for $\Delta = -1 + \sqrt{(1 + 2r)}$ and $r = \frac{1}{2}, \frac{3}{4}, 1$ and $\frac{4}{3}$. The dimensionless measure of wall geometry Δ is the ratio of the distance between wall particles to the diameter of wall particles. For a fixed value of diameter for wall particles the boundary becomes rougher as the distance between wall particles increases. This results, consequently, in a less slip work ($\mathbf{M}\cdot\mathbf{v}$) as well as fewer circumstances under which the boundary supplies energy. Therefore, the downshift in the critical curves is found by comparing Figure 6 with Figure 7.

4.2. The effect of coefficient of restitution e on flows

The most systematic approach in formulating theories for dry rapid granular flows has been to extend the methods employed in developing the kinetic theory of dense gases. One major difference between granular materials and gas molecules is that the collisions between granular materials are inelastic. This implies that the dissipation of kinetic energy due to inelastic collisions plays an important role in the balance of kinetic energy. The coefficient of restitution

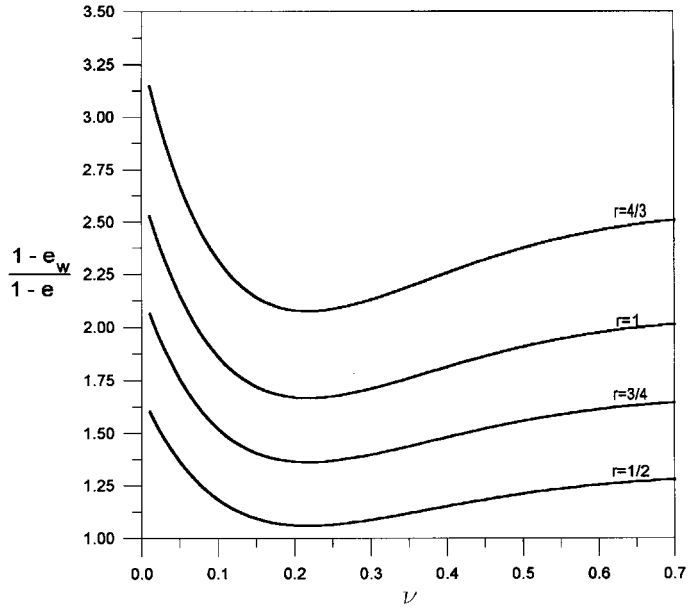

Figure 7. The dependence of the ratio $(1 - e_w)/(1 - e)$ on v for $\Delta = -1 + \sqrt{(1 + 2r)}$ and $r = \frac{1}{2}, \frac{3}{4}, 1$ and $\frac{4}{3}$

e characterizes the inelastic collision between flow particles. In general, the coefficient of restitution e can vary from zero to one. For values of coefficient of restitution that are less than one, kinetic energy is dissipated in a collision. Here and in what follows, the parameters are set to $\bar{v}_f = 0{\cdot}33$ and $\bar{v}_s = 0{\cdot}57$, whenever they are not otherwise specified.

Figures 8–10 show the variations of the solid fraction v, non-dimensionalized granular temperature w and non-dimensionalized mean velocity u with non-dimensionalized distance from the free surface y for $\Delta = 0$, $r = 1$, $e_w = 0{\cdot}8$, $\phi = 12^\circ$ and $e = 0{\cdot}85, 0{\cdot}89, 0{\cdot}92$. From equation (20), the values of λ^2 for $\phi = 12^\circ$ and $e = 0{\cdot}85$, $0{\cdot}89$, $0{\cdot}92$, are equal to $0{\cdot}099$,, $0{\cdot}057$ and $0{\cdot}026$, respectively. Positive λ^2 implies that the energy dissipation that occurs due to an inelastic binary collision between flow particles is greater than the stress power, therefore, the boundary should supply energy in order to maintain a steady gravity-driven granular flow. The values of $(1 - e_w)/(1 - e)$ for $e_w = 0{\cdot}8$ and $e = 0{\cdot}85, 0{\cdot}89, 0{\cdot}92$ are equal to $1{\cdot}33$, $1{\cdot}82$, and $2{\cdot}5$, respectively. From Figure 6, it is found that none of the circumstances under which these boundaries absorb energy from the flow for the full range of solid fractions and $r = 1$. Consequently, the direction of the energy flux is from the boundary to the flow, and this trend is shown in Figure 9. An increase in the coefficient of restitution e corresponds to a decrease in the inelasticity of binary flow particle collisions. This results in less energy dissipation per collision between flow particles. More frequent binary collisions are necessary in order to maintain a steady gravity-driven flow and hence, the depth of flow increases. This phenomenon is demonstrated in Figures 8–10. In the bottom region of the amorphous (or glassy) solid-like granular material, we assume that the mean velocity gradient vanishes but collisions between particles may persist. Consequently, Figure 10 demonstrates that the velocity profile exhibits discontinuity in the slope.

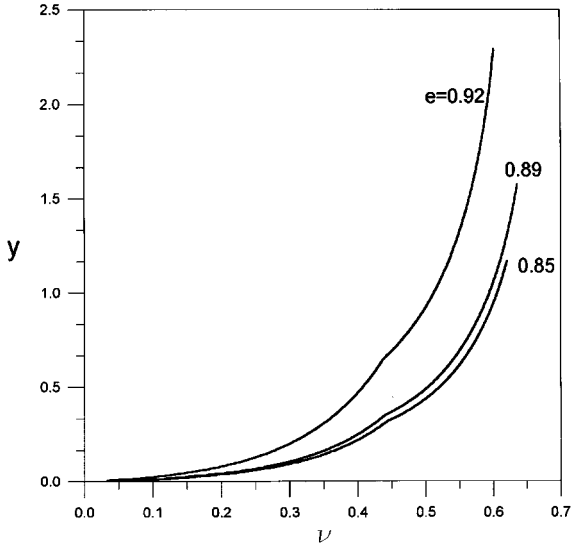

Figure 8. The variation of the solid fraction v with dimensionless distance from the free surface y for $e_w = 0{\cdot}8$, $r = 1{\cdot}0$, $\Delta = 0$, $\phi = 12^\circ$, $\bar{v}_f = 0{\cdot}33$, $\bar{v}_s = 0{\cdot}57$ and $e = 0{\cdot}85$, $0{\cdot}89$ and $0{\cdot}92$

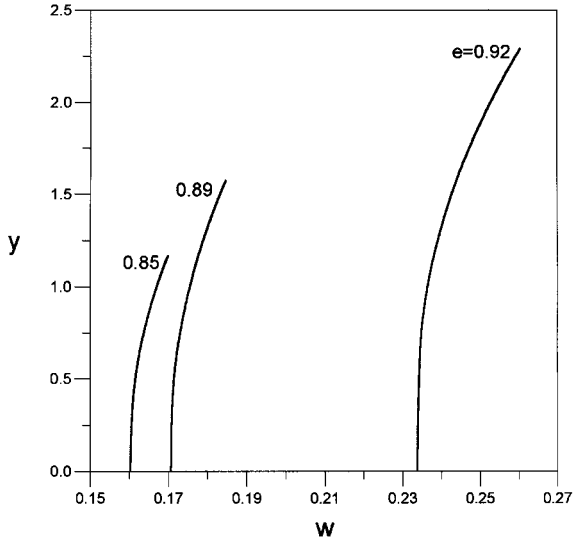

Figure 9. The variation of the non-dimensionalized granular temperature w with dimensionless distance from the free surface y for $e_w = 0{\cdot}8$, $r = 1{\cdot}0$, $\Delta = 0$, $\phi = 12^\circ$, $\bar{v} = 0{\cdot}33$, $\bar{v}_s = 0{\cdot}57$ and $e = 0{\cdot}85$, $0{\cdot}89$ and $0{\cdot}92$

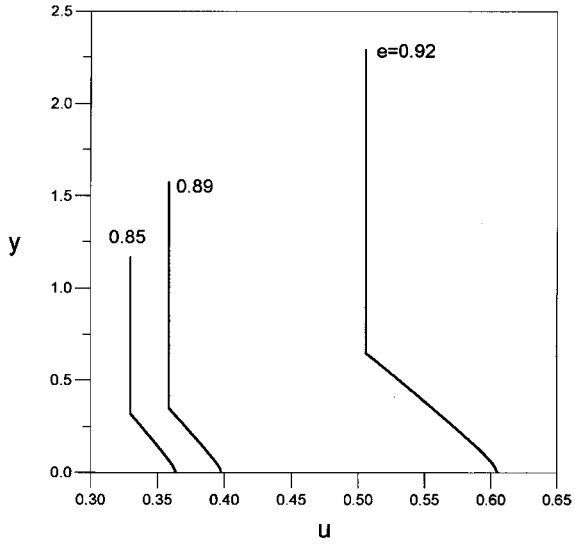

Figure 10. The variation of non-dimensionalized mean velocity u with dimensionless distance from the free surface y for $e_w = 0{\cdot}8$, $r = 1{\cdot}0$, $\Delta = 0$, $\phi = 12^\circ$, $\bar{\nu}_f = 0{\cdot}33$, $\bar{\nu}_s = 0{\cdot}57$ and $e = 0{\cdot}85$, $0{\cdot}89$ and $0{\cdot}92$

4.3. The effect of boundary on flows

For a fixed dimensionless mass flow rate $\dot{m} = 1{\cdot}1$, the behaviour of granular flows of identical smooth spheres with a coefficient of restitution $e = 0{\cdot}92$ depends entirely on the boundary conditions. Figures 11–13 show the variations of the solid fraction ν, non-dimensionalized granular temperature w and non-dimensionalized mean velocity u with non-dimensionalized distance from the free surface y for two cases: (1) at $e_w = 0{\cdot}8$, $r = 1{\cdot}0$, $\Delta = 0$ and $\phi = 13^\circ$; (2) at $e_w = 0{\cdot}683$, $r = 0{\cdot}5$, $\Delta = -1 + \sqrt{(1 + 2r)}$ and $\phi = 23^\circ$.

In case (1), the values of λ^2 for $\phi = 13^\circ$ and $e = 0{\cdot}92$ are equal to $0{\cdot}016$ and positive λ^2 implies that the boundary should supply energy to the flows. The value of $(1 - e_w)/(1 - e)$ for $e_w = 0{\cdot}8$ and $e = 0{\cdot}92$ is equal to $2{\cdot}5$ and from Figure 6, it is found that none of the circumstances under which the boundary absorbs energy from the flow for the full range of the solid fraction and $r = 1$. Consequently, the direction of energy flux is from the boundary to the flow.

In case (2), the values of λ^2 for $\phi = 23^\circ$ and $e = 0{\cdot}92$ are equal to $-0{\cdot}146$ and negative λ^2 implies that the energy dissipation which occurs due to an inelastic binary collision between flow particles is smaller than the stress power, therefore, the boundary should absorb energy in order to maintain a steady gravity-driven granular flows. The value of $(1 - e_w)/(1 - e)$ for $e_w = 0{\cdot}683$ and $e = 0{\cdot}92$ is equal to $3{\cdot}96$, and from Figure 7, it is found that none of the circumstances under which the boundary supplies energy to the flow for the full range of the solid fraction and $r = 0{\cdot}5$. Consequently, the direction of the energy flux is from the flow to the boundary. The variation for granular temperature w with y for both cases is shown in Figure 12. Ahn *et al.*,[31] Richman and Marciniec[30] and Chou[1] all demonstrated that the boundary can either supply energy to the flows or absorb energy from the flows.

The gravity-driven flows shown in Figure 1 consist of a bottom region of amorphous solid-like granular material (passive layer) interacting with a top region of rapidly agitated grains (active

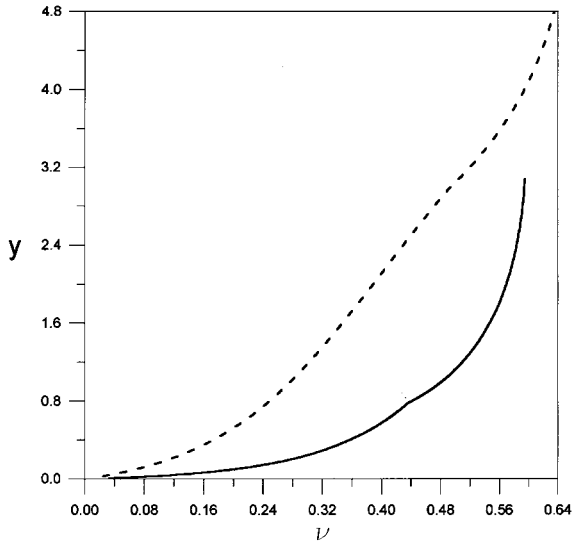

Figure 11. The variation of the solid fraction v with dimensionless distance from the free surface y for $\dot{m} = 1{\cdot}1$, $\bar{v} = 0{\cdot}33$, $\bar{v}_s = 0{\cdot}57$ and $e = 0{\cdot}92$. Solid and dashed lines denote, respectively: $e_w = 0{\cdot}8$, $r = 1{\cdot}0$, $\Delta = 0$, $\phi = 13^\circ$; $e_w = 0{\cdot}683$, $r = 0{\cdot}5$, $\Delta = -1 + \sqrt{(1 + 2r)}$ and $\phi = 23^\circ$

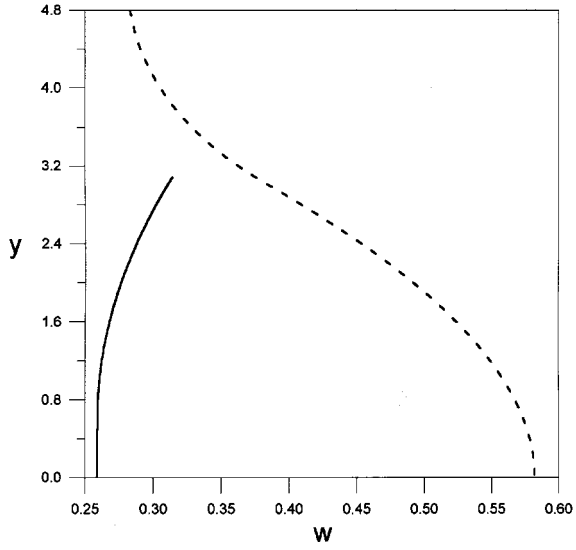

Figure 12. The variation of non-dimensionalized granular temperature w with dimensionless distance from the free surface y for $\dot{m} = 1{\cdot}1$, $\bar{v} = 0{\cdot}33$, $\bar{v}_s = 0{\cdot}57$ and $e = 0{\cdot}92$. Solid and dashed lines denote, respectively: $e_w = 0{\cdot}8$, $r = 1{\cdot}0$, $\Delta = 0$, $\phi = 13^\circ$; $e_w = 0{\cdot}683$, $r = 0{\cdot}5$, $\Delta = -1 + \sqrt{(1 + 2r)}$ and $\phi = 23^\circ$

layer). The flow depth for the fluid-like region is β_f, the flow depth for the solid-like region is β_s and the total flow depth β is the sum of β_f and β_s. The non-dimensionalized flow depths for both cases are: case (1) with chute inclination $\phi = 13^\circ$, $\beta_f = 0{\cdot}78$ for the active layer, $\beta_s = 2{\cdot}3$ for the passive layer and the flow looks like a plug flow; case (2) with chute inclination $\phi = 23^\circ$, $\beta_f = 3{\cdot}0$

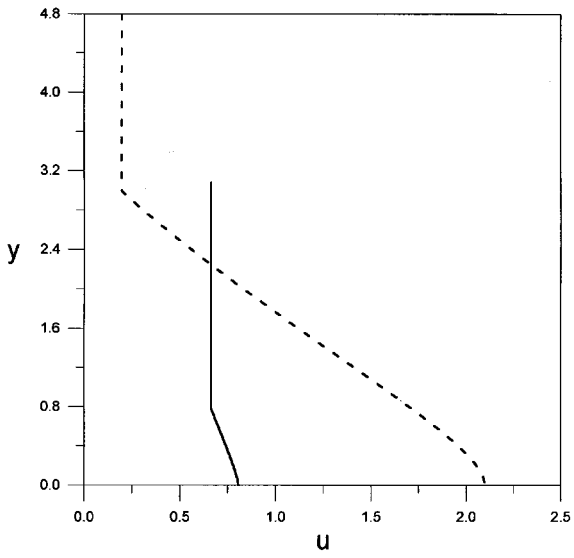

Figure 13. The variation of non-dimensionalized mean velocity u with dimensionless distance from the free surface y for $\dot{m} = 1{\cdot}1$, $\bar{\nu} = 0{\cdot}33$, $\bar{\nu}_s = 0{\cdot}57$ and $e = 0{\cdot}92$. Solid and dashed lines denote, respectively: $e_w = 0{\cdot}8$, $r = 1{\cdot}0$, $\Delta = 0$, $\phi = 13^\circ$; $e_w = 0{\cdot}683$, $r = 0{\cdot}5$, $\Delta = -1 + \sqrt{(1 + 2r)}$ and $\phi = 23^\circ$

for the active layer, $\beta_s = 1{\cdot}8$ for the passive layer and the flow is agitated as well as dilated. The higher the angle of chute inclination, the deeper the granular flow, but the greater the velocity gradient. These are consistent with a physical understanding of the chute flows and are demonstrated in Figures 11 and 13.

4.4. The transitional flows

Ahn *et al.*,[31] found a transitional-type flow in which the granular temperature first increases with distance from the wall boundary (i.e. The boundary absorbs the energy from the flows), then decreases at larger distances from the wall and then becomes uniform near the free surface. On the other hand, Chou[1] found another kind of transitional flows in which the granular temperature first decreases with distance from the wall boundary (i.e. The boundary supplies the energy to the flows), then increases at the interface and then monotonically increases from the interface to the free surface. Under this circumstance, both the active layer and the boundary supply energy to the passive layer. This results in a deeper flow depth for the passive layer. These results qualitatively agree with the numerical simulation by Campbell *et al.*,[43] However, Richman and Marciniec[30] did not discuss the transitional flows.

5. CONCLUSION

Based upon the model of Chou,[1] a steady, inhomogeneous, fully developed, gravity-driven granular flow of identical, smooth, nearly elastic spheres down bumpy inclined surfaces was analysed. The flows consisted of a bottom region of an amorphous solid-like granular material

(passive layer) interacting with a top region of rapidly agitated grains (active layer). The effects of the inclination and coefficient of restitution on the flows and the variations of the energy flux with the boundary geometry were investigated. The smoother the boundary, the greater slip work ($\mathbf{M} \cdot \mathbf{v}$), and the greater circumstances under which the boundary supplies energy. An increase in the coefficient of restitution e results in an increase in the flow depth. The higher the angle of chute inclination, the deeper the depth of granular flow as well as the greater velocity gradient. The research work reported here provides additional theoretical knowledge about chute flows to workers in this field, and also enhances the application of kinetic theory to rapid dry granular flows.

ACKNOWLEDGEMENTS

This research was partially sponsored by a grant, NSC 84-2212-E-020-002 from the National Science Council, Republic of China.

REFERENCES

1. C. S. Chou, 'Studies of granular flows down inclined bumpy surfaces', *J. Chinese Soc. Mech. Engng*., **15**(2)**,** 152–162 (1994).
2. J. T. Jenkins and M. W. Richman, 'Grad's 13-moment system for a dense gas of inelastic spheres', *Arch. Rational Mech. Anal*., **87,** 355–377 (1985).
3. M. W. Richman, 'Boundary conditions based upon a modified Maxwellian velocity distribution for flows of identical, smooth, nearly elastic spheres', *Acta Mech*., **75,** 227–240 (1988).
4. J. T. Jenkins and E. Askari, 'Boundary conditions for granular flows: phase interfaces', *J. Fluid Mech*., **223,** 497–508 (1991).
5. S. B. Savage, 'The mechanics of rapid granular flows', *Adv. Appl. Mech*., **24,** 289–366 (1984).
6. M. W. Richman, 'Kinetic theories for rate dependent granular flows', In J. P. Lamb (ed.), *Proc. US Natl. Congr. Appl., Mech. 10th Austin, Tex*., New York, 1986, pp. 339–346.
7. C. S. Campbell, 'Rapid granular flows', *Ann Rev. Fluid Mech*., **22,** 57–92 (1990).
8. P. K. Haff, 'A physical picture of kinetic granular fluids', *J. Rheol*., **30**(5)**,** 931–948 (1986).
9. J. T. Jenkins, 'Rapid flows of granular material', In R. J. Knops and A. A. Lacey (eds.), *Non-Classical Continuum Mechanics: Abstract Techniques and Applications*, Cambridge University Press, Cambridge, 1987.
10. K. Hutter and K. R. Rajagopal, 'On flows of granular materials', *Continuum Mech. Thermodyn*., **6,** 81–139 (1994).
11. K. Takahasi, 'On the dynamical properties of granular mass', *Geophys. Mag*., **11,** 165–175 (1937).
12. R. A. Bagnold, 'Experiments on gravity-free dispersion of large-solid spheres in a Newtonian fluid under shear', *Proc. Roy. Soc. London*, Ser. A, **255,** 49–63 (1954).
13. D. A. Augenstein and R. Hogg, 'An experimental study of dry powders on inclined surfaces', *Powder Technol*., **19,** 205–215 (1978).
14. O. Hungr and N. R. Morgenstern, 'Experiments on the flow behavior of granular materials at high velocity in an open channel', *Geotechnique*, **34,** 405–413 (1984).
15. H. Ahn, C. E. Brennen and R. H. Sabersky, 'Experiments on chute flows of granular materials', in M. Satake and J. T. Jenkins (eds), *Micromechanics of Granular Materials*, Elsevier, Amsterdam, 1988, pp. 339–348.
16. H. Ahn, C. E. Brennen and R. H. Sabersky, 'Measurements of velocity, velocity fluctuation, density, and stresses in chute flows of granular materials', *J. Appl. Mechs*., **58,** 793–803 (1991).
17. P. C. Johnson, P. Nott and R. Jackson, 'Frictional-collisional equations of motion for particulate flows and their applications to chutes', *J. Fluid Mech*., **210,** 501–535 (1990).
18. T. G. Drake, 'Granular flow: physical experiments and their implications for microstructural theories', *J. Fluid Mech*., **225,** 121–152 (1991).
19. M. Ishida and T. Shirai, 'Velocity distributions in the flow of solid particles in an inclined open channel', *J. Chem. Engng. Jpn*., **12**(1)**,** 46–50 (1979).
20. V. N. Dolgunin and A. A. Ukolov, 'Segregation modeling of particle rapid gravity flow', *Powder Technol*. **83,** 95–103 (1995).
21. P. Nott and R. Jackson, 'Frictional-collisional equation of motion for granular materials and their application to flow in aerated chutes', *J. Fluid Mech*., **241,** 125–144 (1992).
22. K. Hutter, T. Koch, C. Pluss and S. B. Savage, 'The dynamics of avalanches of granular materials from initiation to runout. part II: Experiments', *Acta Mech*., **109,** 127–165 (1995).

23. A. W. Roberts, 'An investigation of the gravity flow of noncohesive granular materials through discharge chutes', *ASME Trans. J. Engng. Ind*., **91,** 373–381 (1969).
24. S. B. Savage, 'Gravity flows of cohesionless granular materials in chutes and channels', *J. Fluid Mech*., **92,** 53–96 (1979).
25. G. Ahmadi and M. Shahinpoor, 'A kinetic model for rapid flows of granular materials', *Int. J. Non-Linear Mech*., **19,** 177–186 (1983).
26. M. Sayed and S. B. Savage, 'Rapid gravity flow of cohesionless granular materials down inclined chutes', *ZAMP*, **34,** 81–100 (1983).
27. D. Ma and G. Ahmadi, 'A turbulence model for rapid flow of granular material Part II. Simple shear flows', *Powder Technol*., **44,** 269–279 (1985).
28. K. Hutter, F. Szidarovsky and S. Yakowitz, 'Plane steady shear flows of a cohesionless granular material down an inclined plane. A model for flow avalanches Part I: Theory', *Acta Mech*., **63,** 87–112 (1986).
29. K. Hutter, F. Szidarovsky and S. Yakowitz, 'Plane steady shear flows of a cohesionless granular material down an inclined plane. A model for flow avalanches Part II: Numerical results', *Acta Mech*., **65,** 239–261 (1986).
30. M. W. Richman and R. P. Marciniec, 'Gravity-driven granular flows of smooth, inelastic spheres down bumpy inclines', *J. Appl. Mech*., **57,** 1036–1043 (1990).
31. H. Ahn, C. E. Brennen and R. H. Sabersky, 'Analysis of fully developed chute flow of granular materials', *J Appl. Mech*., **59,** 109–119 (1992).
32. P. K. Haff, 'Grain flow as a fluid-mechanical phenomenon', *J. Fluid Mech*., **134,** 401–430 (1983).
33. J. W. Nunziato and S. L. Passman, 'Gravitational flows of granular materials with incompressible grains', *J. Rheol*. **24**(4)**,** 395–420 (1980).
34. K. G. Anderson and R. Jackson, 'A comparison of the solution proposed equations of motion of granular materials for fully developed flow down inclined planes', *J. Fluid Mech*., **241,** 145–168 (1992).
35. S. B. Savage and K. Hutter, 'The motion of a finite mass of granular material down a rough incline', *J. Fluid Mech*., **199,** 177–215 (1989).
36. S. B. Savage and K. Hutter, 'The dynamics of avalanches of granular materials from initiation to runout. part I: Analysis', *Acta Mech*., **86,** 201–223 (1991).
37. K. Hutter, 'A continuum model for finite mass avalanches having shear-flow and plug-flow regime', *Internal Report*, Federal Institute of Snow and Avalanches Research, Weissfluhjoch, CH-7620 Davos, 1989.
38. R. M. Lang, 'An experimental and analytical study on gravity-driven free surface flows of cohesionless granular media', *Doctoral Diss*., Techn. Hochschule Darmstadt, Germany, 1992.
39. R. Perla, T. T. Cheng and D. M. McClung, 'A two parameters model of snow avalanche motion', *J. Glaciol*. **26,** 197–207 (1980).
40. H. Norem, F. Irgens and B. Schielhop, 'A continuum model for calculating snow avalanche', In B. Salm, and H. U. Gubler (eds.), *Avalanche formation, movement and effects*, vol. **162,** IAHS Publ., 1987, pp. 363–379.
41. K. R. Rajagopal and R. Gudhe, 'Stability analysis for the flow of granular materials down an inclined plane using kinetic model', *Fifth NSF-DOE workshop on Flow of Particulates and Fluids*, Cornell, 1993.
42. C. S. Campbell and C. E. Brennen, 'Chute flows of granular material: some computer simulations', *Trans. ASME*, **52,** 172–178 (1985).
43. C. S. Campbell and C. E. Brennen and R. H. Sabersky, 'Flow regimes in inclined open-channel flows of granular materials', *Powder Technol*., **41,** 77–82 (1985).
44. O. R. Walton, R. L. Braun, R. G. Mallon and D. M. Cervelli, 'Particle-dynamics calculations of gravity flow of inelastic, frictional spheres', in M. Satake and J. T. Jenkins (eds), *Micromechanics of Granular Materials*, Elsevier, Amsterdam, 1988, pp. 153–162.
45. H. Norem, F. Irgens and B. Schielhop, 'Simulation of snow avalanche flow in runout zones', *Ann. Glaciol*. **13,** 218–225 (1989).
46. F. Szidarovszky, K. Hutter and S. Yakowitz, 'A numerical study of steady plane granular chute flows using the Jenkins-Savage model and its extension', *Int. J. Numer. Mech. Engng*., **24,** 1993–2015 (1987).
47. F. Reif, *Fundamentals of Statistical Mechanics and Thermal Physics*, McGraw-Hill, New York, 1965.
48. J. T. Jenkins and S. B. Savage, 'A theory for the rapid flow of identical, smooth, nearly elastic, spherical particles', *J. Fluid Mech*., **130,** 187–202 (1983).
49. L. Verlet and D. Levesque, 'Integral equations for classical fluids III. The hard discs system', *Mol. Phys*., **46,** 969–980 (1982).

